

Vital Protocol for Reliability and Accuracy of PolyWare™ Measurements

Jong Min Lee

Catholic University of Daegu

Seung-Hoon Baek

Kyungpook National University Hospital

Yeon Soo Lee (✉ biomechanics.yslee@gmail.com)

Catholic University of Daegu

Research Article

Keywords: Total Hip Arthroplasty (THA), PolyWare (PW), Polyethylene Wear, Anteversion, Lateral inclination

Posted Date: March 15th, 2021

DOI: <https://doi.org/10.21203/rs.3.rs-142211/v2>

License: © ⓘ This work is licensed under a Creative Commons Attribution 4.0 International License.

[Read Full License](#)

Vital Protocol for Reliability and Accuracy of PolyWare™ Measurements

¹Jong Min Lee, ²Seung-Hoon Baek, ¹Yeon Soo Lee

¹ Department of BioMedical Engineering, School of BioMed Science, Catholic University of Daegu, Gyungbuk, Rep. Korea 38430

² Department of Orthopaedic Surgery, School of Medicine, Kyungpook National University, Kyungpook National University Hospital, Daegu, Rep. Korea 41944

Corresponding author: Yeon Soo Lee, Ph.D.

Dept. of Biomedical Engineering, College of Medical Science, Catholic University of Daegu, Hayangro 13-13, Hayang-Eup, Gyongsan-Si, Gyongsangbuk-do, Rep. OF Korea, Zip 38430

Office: +82-53-850-2514, Fax: +82-53-359-6754

biomechanics.yslee@gmail.com

Abstract

Introduction: PolyWare™ software (PW) has been an exclusively used software in most polyethylene wear studies of total hip arthroplasty (THA). We found that PolyWare™ (PW) measurements can be significantly inaccurate and unrepeatable depending on imaging conditions or subjective manipulation choices. In this regard, this study reveals the required conditions to achieve the best accuracy and reliability of the PW measurements.

Results: Among all the imported X-ray images, those with a resolution of 1076×1076 exhibited the best standard deviation in wear measurements as small as 0.01 mm and the least occurrences of blurriness. The edge detection area specified as non-squared and off the femoral head center exhibited the most occurrence of blurriness. At the X-ray scanning moment, an eccentric placement of the femoral head center by 15 cm superior to the X-ray beam center led to an acetabular anteversion measurement error up to 5.3°.

Conclusion: Because PW has been an exclusively used polyethylene wear measurement tool, revealing its error sources and making the countermeasure are of great importance. The results request researchers to observe the following conditions; 1) the original X-ray image be 1076×1076 squared X-ray images, 2) the edge detection area be specified as a square with edge lengths of 5 times the diameter of the femoral head centered at the femoral head center, 3) the femoral head center or acetabular center be placed as close to the center line of the X-ray beam as possible, at the X-ray scanning moment.

Key Words: Total Hip Arthroplasty (THA); PolyWare (PW); Polyethylene Wear; Anteversion; Lateral inclination

1. Introduction

Wear debris-induced osteolysis and implant loosening are the primary causes limiting longevity after total hip arthroplasty (THA)^{1,2}. Additionally, proper placement of the acetabular cup (AC) in THA is essential to reduce wear and dislocation. Thus, early detection of the complications via accurate measurement of wear rate and AC alignment during regular check-up is of significant clinical importance³⁻⁸.

Previous studies demonstrated higher accuracy of PW in measuring wear rate and cup position relative to other software or methods⁹. Even though reliable interactive computerized methods using 2D AP X-ray image or 2D-3D registration algorithm were proposed for the measurements^{7,10}, most of them have not been commercialized. In contrast, PolyWareTM software (PW) has been an exclusively used commercialized tool for THA polyethylene wear measurement for several, due to ease of operation, no need of bead implantation or dual X-ray scanners. Because PW constructs sphere models representing AC and femoral head (FH) for matching them onto silhouettes of them on X-ray images, it can measure the anteversion and the lateral tilt of AC beside polyethylen wear.

However, we authors found that PW measurement results can be significantly inaccurate depending on factors such as the observer's technical preferences and features of X-ray images. During PW operation, various error messages are frequently encountered due to unknown causes, and PW then spontaneously turns off in the middle of measurements. From the error situations, the current authors noticed following errors of PW that can be minimized by manipulating observer's choices or skill; *Ext1*) PW's extrinsic error due to inappropriate size of the original X-ray images imported; *Ext2*) PW's extrinsic error due to eccentric location of the object away from the X-ray source-to-detector center line; *Int1*) PW's intrinsic error, i.e. the PW's functional limitation that cannot fix the measurement error due to the asymmetric specification of edge detection area.

Because PW has been an exclusively used polyethylene wear measurement tool, revealing its errors sources and making the countermeasure are of great importance. In this regard, the current study has two aims. The first is to experimentally assess PW's three extrinsic and intrinsic errors (*Ext1*, *Ext2* and *Int1*). The second is to provide three technical guidelines on which clinicians and researchers can manipulate for measurement improvement.

2. RESULTS

2.1. Image loading error vs loaded image size

With respect to the image loading error, images with a resolution equal or higher than 1800×1800

frequently failed while loading the initial or final X-ray images (Table 1). Each resolution image was tested ten times. All the images of resolutions corresponding to 2494×2494, 2780×2780, or 3020×3020 failed at being loaded into PW, i.e., the loading error ratio = 10/10 = 1. 1800×1800 resolution images showed an image loading error at a ratio of 8/10. Conversely, all the images with a resolution of 1500×1500 or lower were successfully loaded into PW without any failure.

Table 1. PolyWare compatibility tests of various TIFF X-ray image sizes

Image	Resolution	1024 1024	1076 ×1076	1200 ×1200	1300 ×1300	1400 ×1400	1500 ×1500	1800 ×1800	2494 ×2494	2780 ×2780	3020 ×3020
	Gray bits	8	8	8	8	8	8	8	8	8	8
	Size (KB)	1,060	1,220	1,499	1,742	1,994	2,253	3,433	5,978	7,202	26,721
Loading Error ratio (in the desktop PC)		0/10	0/10	0/10	0/10	0/10	0/10	8/10	10/10	10/10	10/10
Loading Error ratio (in the laptop PC)		0/10	0/10	0/10	0/10	0/10	0/10	8/10	10/10	10/10	10/10
Blur ratio in the edge detection image (identical in both PCs)		5/10	2/10	4/10	6/10	5/10	5/10	2/2	NA	NA	NA
Wear (mm) True= 6.67 of All cases		6.88 (0.50)	6.79 (0.01)	6.42 (0.42)	6.64 (0.52)	6.70 (0.14)	6.61 (0.29)	6.49 (0.66)	NA	NA	NA
Wear (mm) True= 6.67 of Non-blur cases only		6.60 (0.00)	6.79 (0.00)	6.24 (0.17)	6.27 (0.28)	6.68 (0.01)	6.46 (0.25)	NA	NA	NA	NA
Lateral tilt (°) True= 36.70° of All cases		36.5(0.8)	36.0 (0.5)	36.5 (0.5)	36.2 (0.4)	36.2 (0.4)	36.4 (0.6)	36.5 (0.9)	NA	NA	NA
Lateral tilt (°) True= 36.70° of Non-blur cases only		36.3 (0.7)	36.0 (0.6)	36.6 (0.6)	36.3 (0.3)	36.0 (0.4)	36.3 (0.4)	NA	NA	NA	NA
Anteversión (°) True=9.0° of All cases		-8.7 (0.4)	-8.6 (0.7)	-8.3 (0.3)	-8.7 (0.8)	-8.8 (0.5)	-8.7 (0.7)	-8.5 (0.1)	NA	NA	NA
Anteversión (°) True=9.0° of Non-blur cases only		-8.5 (0.2)	-8.6 (0.8)	-8.5 (0.2)	-8.9 (0.9)	-9.0 (0.5)	-8.5 (0.7)	NA	NA	NA	NA

(Note) NA=Not available since none of the measurement trials was successful or possible. The wear, lateral tilt,

and anteversion were obtained from only the successful measurements without any blur phenomenon in both the initial and final images. These tests were performed for the X-ray image whose center coincides with the center of femoral head (O in Fig 8).

The image loading error was identical for the desktop PC and laptop PC in terms of occurring condition or occurrence ratio of the image loading error (Table 1). Hence, PW image loading error did not depend on computer performance.

2.2. Blur of the edge detection image vs loaded image size

Only the images successfully loaded into PW can be proceeded to the edge detection process. For all the images successfully loaded into PW, edge detection area was specified in the head-centered $5D_h \times 5D_h$ square.

All the two successfully loaded 1800×1800 resolution images became blurred when the edge detection area specified error (Table 1). In contrast, images with a resolution of 1076×1076 exhibited a 2/10 blur ratio, which corresponded to the least blur occurrence ratio among all resolutions.

2.3. PW compatible geographical features of the edge detection area specification

The effects of the edge detection area's geographical feature were assessed only with X-ray images with a resolution of 1076×1076 , because all the images with the aforementioned resolution were successfully loaded into PW and exhibited the least blur in the edge detection process. The occurrence ratio of the blur was quantified as incidence over 10 trials. The blur indicates that the original image is degraded by the blur created while specifying the edge detection area, and edge detection will be processed for the degraded image.

The reliability of measurements was evaluated by the incidence of blurs or unexpected errors, as in Table 2. When the edge detection area was specified as a square with its center located at the center of FH on X-ray images, PW measurements exhibited higher reliability than when the center of the area was specified as randomly located off the center of FH. The unexpected error indicates the edge detection procedure returned an error message without any explanation and terminates the edge detection operation.

Ten trials of the not head-centered non-squared specification resulted in three unexpected errors and five blurs at the edge detection procedure. When it comes to blurring, the $7D_h \times 7D_h$ square specification exhibited two blur incidents in ten trials, while $5D_h \times 5D_h$ square specification exhibited one blur incident in 10 trials. Wear

values of both square specifications (including all the blur and non-blur cases) corresponded to 6.79(0.00) mm, which was extremely close to the true value of 6.67 mm. In contrast, ten trials of not head-centered non-squared specification resulted in three unexpected errors and five blurs at the edge detection procedure. The wear of the not head-centered random non-square specification was 6.92(0.15) mm, which was less accurate and less precise than the squared specifications.

Table 2. The measured wear for different area specifications (True wear= 6.67 mm)

Trials	Head-centered				Not head-centered	
	5D _h ×5D _h square		7D _h ×7D _h square		Non-square	
	Trouble	Wear (mm)	Trouble	Wear (mm)	Trouble	Wear (mm)
1	No	6.79	No	6.79	No	7.05
2	Blur	7.76	No	6.79	Error	NA
3	No	6.79	No	6.79	Blur	7.75
4	No	6.79	No	6.79	No	6.79
5	No	6.79	No	6.79	Blur	6.12
6	No	6.79	Blur	6.12	Error	NA
7	No	6.79	Blur	6.12	Blur	7.98
8	No	6.79	No	6.79	Blur	6.12
9	No	6.79	No	6.79	Error	NA
10	No	6.79	No	6.79	Blur	6.12
Total	Error: 0 Blur: 1	6.89(0.31) of all 6.79(0.00) of 9 N-blurs 7.76 of 1 blur	Error: 0 Blur: 2	6.66(0.28) of all 6.79(0.00) of 8 N-blurs 6.12(0.00) of 2 blurs	Error: 3 Blur: 5	6.85(0.79) of all 6.92(0.18) of 2 N-blurs 6.82(0.96) of 5 Blurs

(Note) NA=Not available since none of the measurement trials was successful or possible. These tests were performed for the X-ray image whose center coincides with the center of femoral head (O in Fig 8). The symbol D_h denotes the diameter of the femoral head component.

2.4. Effect of the prosthesis’s eccentric location at the X-ray scanning moment

The eccentricity tests were performed with only the images with a resolution of 1076×1076, and their edge detection area specification was the head-centered 5D_h×5D_h square. The PW measurements for each eccentricity mode were averaged from ten trials. Table 3 shows the wear amount and alignment measurement results for the nine different eccentricity modes.

The spatial eccentricity of the prosthesis from the original X-ray image center led to inaccurate results in wear measurement. L_{15} , $R_{15}S_{15}$, $R_{15}I_{15}$, and $L_{15}I_{15}$ eccentricities resulted in an error of approximately 0.42 mm, and the I_{15} eccentricity resulted in an error of approximately 0.67 mm. $L_{15}S_{15}$ and R_{15} resulted in an error of 0.50 mm.

The AC anteversion became considerably inaccurate due to any eccentricity along with all directions,

and the maximum error appeared, especially at $L_{15}I_{15}$ mode by 5.4° ($= 14.4^\circ - 9.0^\circ$). S_{15} and I_{15} eccentricity modes resulted in a higher anteversion measurement by 4.3° and a lower anteversion by 3.6° , respectively.

Table 3. PloyWare measurement results for nine spatial eccentricity modes

Eccentricity mode	Liner wear, <i>mm</i> True=6.67	Lateral tilt, $^\circ$ True=36.7	Anteversion, $^\circ$ True=-9.0
O	6.79(0.00)	36.3(0.3)	9.0(0.6)
L_{15}	6.25(0.00)	36.2(0.6)	11.1(0.7)
$L_{15}S_{15}$	6.52(0.00)	36.2(0.2)	7.9(0.6)
S_{15}	6.79(0.00)	36.7(0.3)	4.7(0.5)
$R_{15}S_{15}$	6.25(0.00)	37.2(0.3)	1.5(0.2)
R_{15}	6.52(0.00)	37.2(0.3)	5.9(0.6)
$R_{15}I_{15}$	6.25(0.00)	37.2(0.3)	9.8(0.4)
I_{15}	6.00(0.00)	37.1(0.5)	12.6(0.4)
$L_{15}I_{15}$	6.25(0.00)	37.2(0.4)	14.4(0.3)

(Note) L, R, S, and I in the eccentricity mode represents left, right, superior, and inferior, respectively. The subscript 15 in the eccentricity mode indicates the translational of 15 mm.

3. DISCUSSION

In the study, we are dealing with a very uncomfortable fact that some of the existing published PW measurement studies could be unreliable if they did not recognize and fix the errors that our research revealed. Based on the results in our study, we suggest polyethylene wear researchers follow the next three PW measurement protocols obtained from our findings.

Finding 1. Optimal size of original X-ray images (S_{best})

With respect to the error in loading images into PW, all images with resolution of 1500×1500 or lower were successfully loaded into PW without any failures. Especially, the images with a resolution of 1076×1076 exhibited two of ten (2/10) blur occurring ratio that was the lowest among all images with various resolutions. In practical situations, an original image transferred from medical modality can be not-squared such as

1076×1500 or 1200×1100. In this case, we recommend cropping it into a squared image centered at the center of the original image and changing its pixel size to 1076×1076. Hence, an X-ray image with resolution of 1076×1076 is optimally compatible with the PW measurement, i.e., $S_{best}=1076\times1076$.

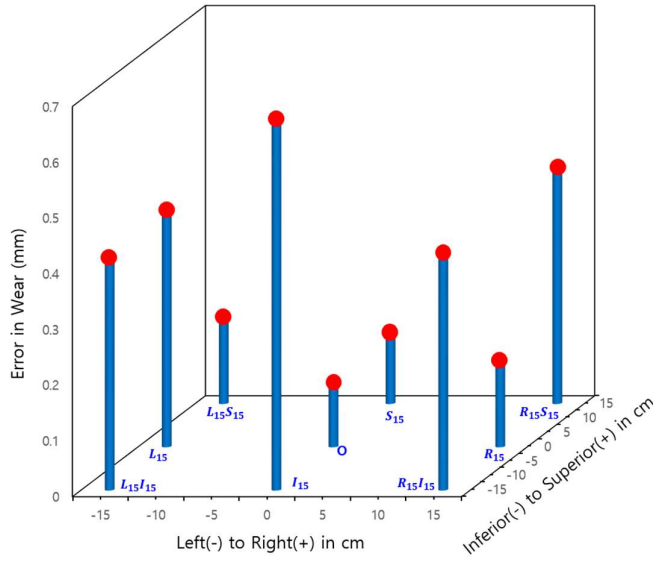


Fig 1. Error (in absolute value) in the wear for spatial eccentricity modes of the femoral head in the original X-ray images

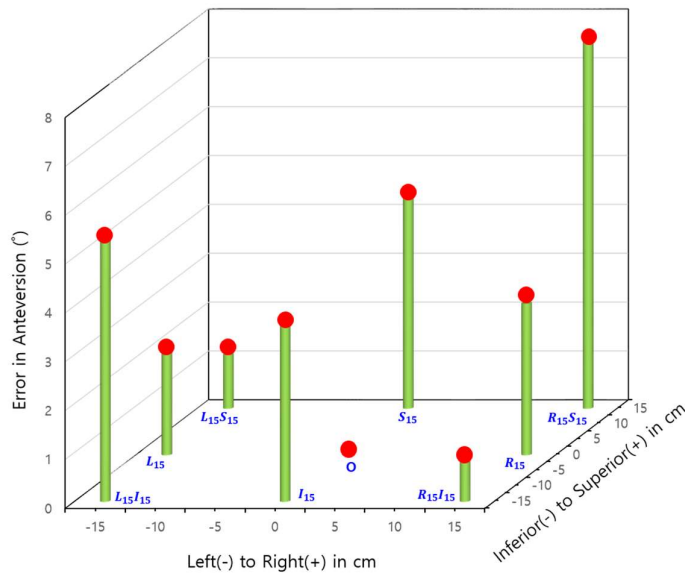


Fig 2. Errors (in absolute value) in the acetabular anteversion for spatial eccentricity modes of the

femoral head in the original X-ray images

Finding 2. Optimal location of the THA prosthesis on the original X-ray images (E_{best})

The eccentricity of FH location from the X-Ray beam center line clearly decreased accuracy in the linear wear and AC anteversion measurements. The errors in Figs. 1 and 2 represent mean deviations from the true wear and anteversion values recalculated from Table 2, respectively. It is clear that an eccentric placement of prosthesis with respect to the X-ray beam center line leads to errors in the linear wear and anteversion of AC. Specifically, the anteversion exhibited a larger error due to the prosthesis placed superiorly or inferiorly away from the X-ray beam source. The anteversion measured by PW was not reliable unless FH was placed extremely close to the central X-ray beam line at the X-ray scanning moment.

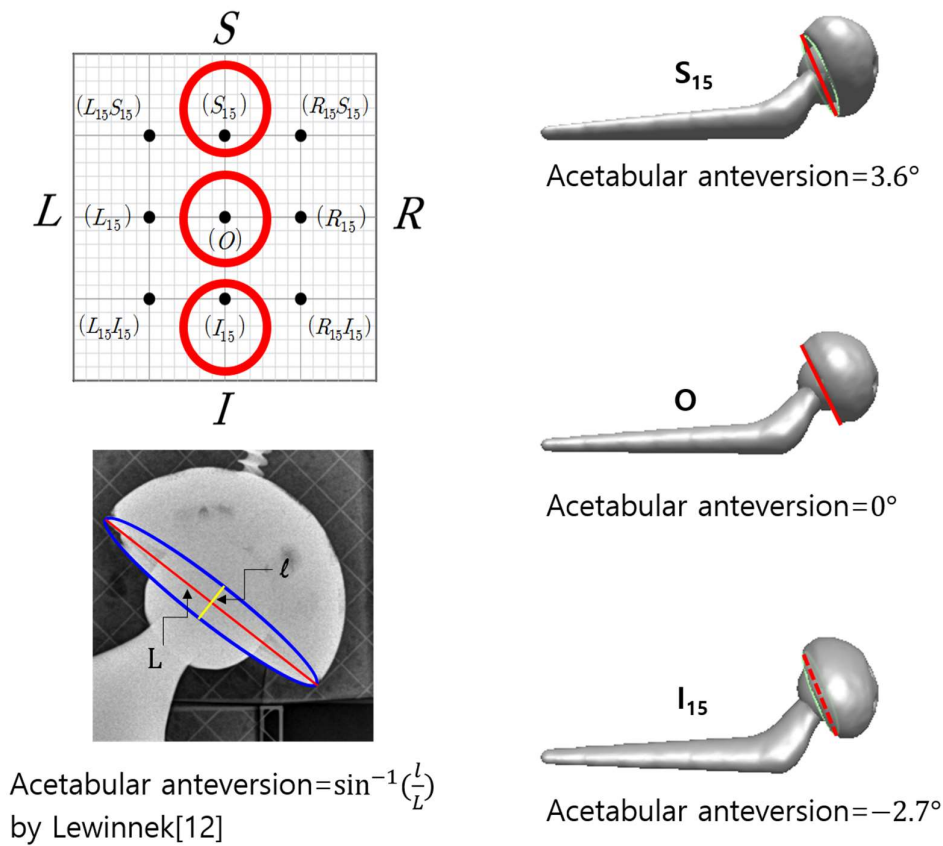


Fig 3. Measurement of acetabular anteversion using a CAD to investigate the effect eccentricity of the prosthesis from the center of X-ray beam on the acetabular anteversion. The same X-ray images used for Polyethylene measurements were also used for the measurement using a CAD software, i.e. Rapidform 2006® (INUSTechnology, Seoul, Korea). The superior and inferior placements of the prosthesis bring about errors in acetabular anteversion, by the nature of perspective X-ray imaging.

In order to assess the reason as to why the eccentric prosthesis placement significantly affected the anteversion, we measured the anteversion of the virtual X-ray images generated by simulating a projection of the hip prosthesis 3D CAD model in a perspective view. The perspective view simulation was made with a 3D CAD software, i.e. Rapidform 2006® (INUSTechnology, Seoul, Korea). Rapidform 2006 makes a virtual perspective view, along a source-to-detector distance of 394 cm, such that a proximal edge of a 100cm × 100cm × 100cm cube placed on the proximal detector plane is projected as 130 cm on the detector plane. Fig. 3 demonstrates changes in linear wear based on superior and inferior eccentricity modes. The anteversion was calculated via the Lewinnek method¹¹. The superior and inferior 15 cm eccentricity modes corresponded to 4.3° of over anteversion and 3.6° of less anteversion, respectively. From our CAD measurement using Rapidform, it is postulated that PW adopts the Lewinnek method for acetabular anteversion calculation. It is concluded that the acetabular measurement is valid only when the center of FH (or similarly the center of AC) is placed very close to the center line of X-ray beam. Hence, the eccentricity significantly deteriorates the accuracy in the wear and acetabular anteversion; thus, placement of the FH center along the center line of the X-ray beam ($E_{best} = 0$) should be complied.

Finding 3. Optimal specification of the edge detection area (G_{best})

The pre-process AP image in PW measurement involves cutting out the unnecessary part from the originally loaded image. The image remaining after the pre-process is used for edge detection of FH and AC. Geographical features of the area as specified by users for the pre-process affected the occurrence of image blur. The geographical features of the selected area include size and symmetry with respect to the center of FH. In the current study, asymmetry of the specified area specification clearly increased the occurrence ratio of blur. And, the head-centered $5D_h \times 5D_h$ square is preferable to the head-centered $7D_h \times 7D_h$ square because the magnified process image can be more precisely analyzed for edge detection. In this regard, we postulate that Head-centered $3D_h \times 3D_h$ square would be also best preferable. The optimal geographical specification mode of the image process for edge detection corresponded to the head-centered $5D_h \times 5D_h$ square, i.e. $G_{best} = \text{Head-centered } 5D_h \times 5D_h \text{ square or probably Head-centered } 3D_h \times 3D_h \text{ square}$.

The current study presents *several limitations*. *First*, the X-ray images used in the study are clinically impractical because the X-ray images are only of prostheses without real tissues such as bones and soft tissues. There should be a small occlusion when tissues do not exist around the prostheses; thus, the outline of the prostheses will be clearer than that when tissues are present around the prostheses. However, the aim of the

current study involves evaluating measurement accuracy. In the evaluation of accuracy, the true value of wear was precisely simulated via a translation, and we compared the measured values with the true value. Real clinical patient hip images are not able to provide true wear since we are not permitted. Additionally, it is difficult to standardize complex shapes and material compositions of human tissue around the THA prostheses at each X-ray scanning, and this disables the accuracy test. Hence, in the current study, the X-ray images were obtained without considering human tissues, in order to precisely manipulate wear simulation via translating the femoral component. In future studies, a simulation may be developed to represent tissues around the prostheses. *Second*, the resolution and aspect ratio of the original X-ray images that were tested did not cover all possible variations. Practical clinical X-ray images might exhibit diverse types of resolutions or aspect ratios. Additionally, practically obtained original X-ray images might not be squared although PW automatically converted the imported images into squared ones. However, the aspect ratio will not matter only if the X-ray image has a resolution of 1500×1500 or lower. *Third*, the current study investigated only one type of THA prostheses, i.e., THA using fourth-generation ceramic-on-polyethylene articulation. When it comes to opacity in X-ray scanning, fourth-generation ceramic-on-polyethylene and metal-on-polyethylene are comparable since their liners are composed of polyethylene. However, if the liners are composed of radio-opaque materials, such as metal or fourth-generation ceramics, it is difficult to distinguish the silhouette of the femoral head from the liners. It is noted that the PW compares patient X-ray images to measure the volume of polyethylene material worn away from bearing surfaces of orthopedic hip implants over time (<http://www.draftware.com/html/polyware.htm>). Hence, PW is feasible only for the wear measurement of Polyethylene.

In the authors' knowledge, there is no published literature that investigated the error sources and their solutions in PW measurement. Recent literature reported that manual measurement on the digital X-ray screen measurements and PW measurement are comparable in the measurement of AC anteverstion^{9,12}. But, it has to be noted that their study reports only repeatability rather than accuracy since there is no way for them to measure true polyethylene wear from living THA patients. When it comes to wear, the comparison of our findings with existing literature is quite limited.

5. Conclusion

Because PW has been an exclusively used polyethylene wear measurement tool, revealing its errors sources and making the countermeasure are of great importance. In order to ensure maximum possible accuracy and reliability in PolyWare™ measurements, it is strongly recommended to follow the methodology proposed in this study. Otherwise, the validity of the measurements cannot be reliable.

6. METHODS

6.1. Study design

The experiments parametrically investigated the effects of three possible factors as error; the size of original X-ray images (S), eccentric positions of the THA implants with respect to the X-ray source-to-detector center line (E), and geographical feature of edge detection area specification (G). The S , E , and G factors correspond to $Ext1$, $Ext2$, and $Int1$, respectively. Fig 4 shows the overall scheme of the current study. Eventually, three best parameters to S , E , and G were determined to secure PW measurements' optimal reliability.

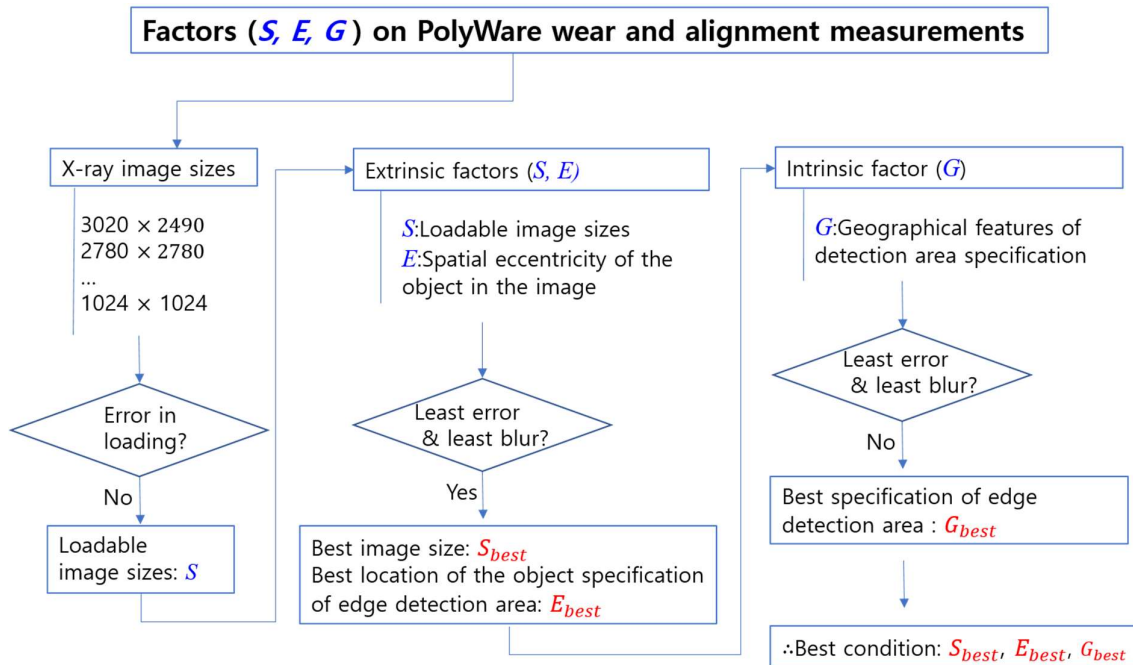


Fig 4. Overall process scheme of the current study

6.2. Materials

THA prosthesis

The used THA prosthesis set was composed of BioloX[®] Delt ϕ 28 mm femoral head (CeramTec[®], Plochingen, Germany), Triology[®] ϕ 58 mm acetabular cup (Zimmer Biomet[®], Warsaw, IN, USA), a Bencox[®] stem (CorenTec[®], Cheon-An, Korea), and a Longevity[®] liner (Zimmer Biomet[®], Warsaw, IN, USA).

Wear measurement software

The evaluated radiographical measurement software was PolyWare™ software v.8 (Draftware Inc., IN, USA). A PW measurement is to compare the analysis results of any two follow-up times. Fig. 5 demonstrates the measurement process scheme of PW. The follow-up times can be postop (1–14 days after THA), 3 months, 6 months, 1 year, and annually thereafter. The results of the analysis include the polyethylene liner wear, and anteversion and lateral inclination of AC. The linear wear is calculated as the change in the distance between FH center and AC center, from the initial to the final follow-up times. In a PW measurement, the initial and final follow-up times correspond to the earlier and later, respectively.

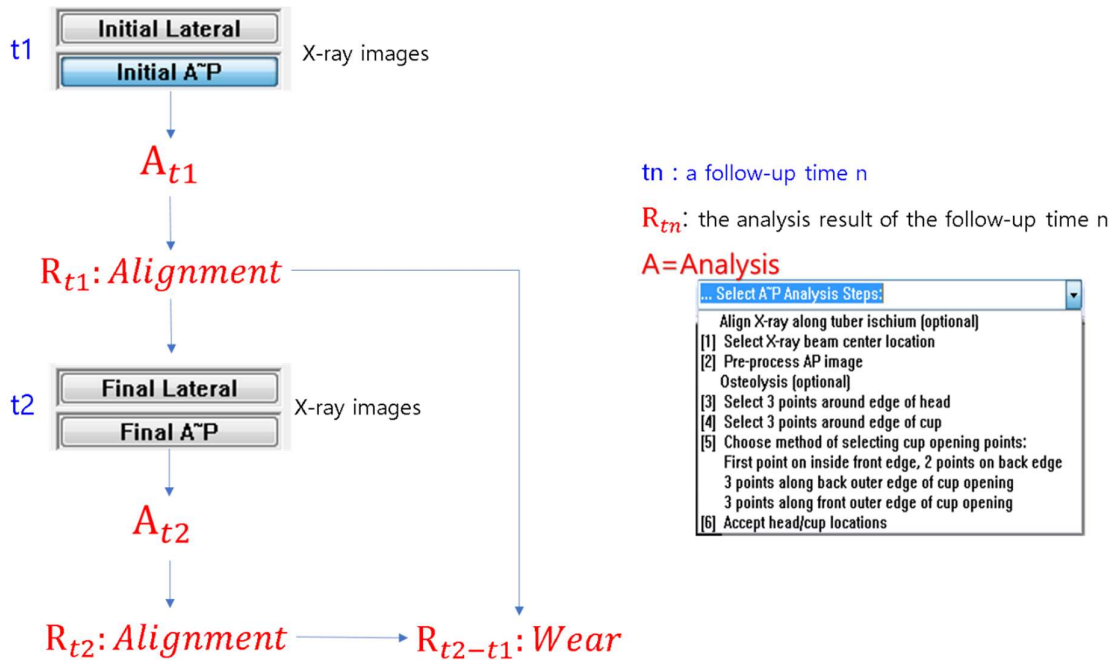


Fig 5. PolyWare work flow

X-ray images

The images of the THA prostheses were obtained by a clinical X-ray scanner (Innovision SH, DongKang Co., Rep. Korea). The perpendicular distance from the X-ray beam source to the detector panel was set to a constant of 115 cm. All X-ray images were originally acquired at a resolution of 3020×3020 pixels in DICOM format. And they were converted into TIFF format since PW software v.8 analyses only TIFF images or automatically converts DICOM images into TIFF ones inside the software.

Computers

Computer performance may affect the error incidence of PW work. In this regard, a laptop personal computer (PC) and a desktop PC with different performances were tested (Table 4).

Table 4. Specifications of the laptop and the desktop personal computers (PCs)

	Manufacturer, Model	OS	RAM	CPU	Memory	Graphics
Laptop PC	Laptop PC NT270E5R, Samsung Electronics Co., Ltd., Suwon, South Korea.	Windows 7 (32bit)	8 GB	Intel Core i5 4200U	DDR 3 8 GB	Intel HD Graphics 4400, Shared memory
Desktop PC	Desktop PC, Custom-built	Windows 10 (64bit)	16 GB	Intel Core i7 4930K	DDR 3 16 GB	NVIDIA GeForce GTX 750, 1GB

Experimental simulation setup of polyethylene wear and AC alignment

Wear was simulated by translating the femoral component. The initial prosthesis position corresponded to the state in which FH fully contacts AC, while the final position was designed as a translation of FH by 6.67 mm along the normal direction to the equatorial plane of AC. Before (initial) and after (final) the translation of the FH component, X-ray images were obtained (Fig. 6). To secure the spatial relationship between FH and AC at the initial and final positions during the X-ray scanning, alginate, i.e. an irreversible hydrocolloid, was used. Alginate powder and water were mixed up in a plastic case. The mixture was kept at rest until the alginate had commenced solidification. Then, the hip prosthesis components were placed over the alginate. In one minute, the alginate foam was firmly solidified to a native shape moulding frame of the prostheses.

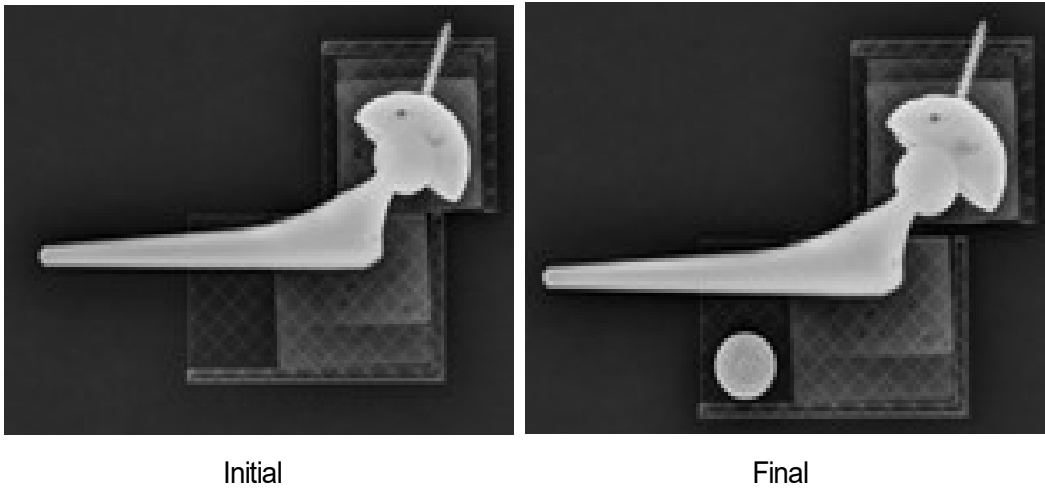


Fig 6. X-ray images of the initial (the left) and final (the right) positions, simulating the wear of the cup by a translation of the femoral stem of 6.67 mm normal to the equator plane of AC.

Measurement of true polyethylene wear and AC alignment

In order to determine the true translation as the simulated wear, a CAD measurement was adopted. The original X-ray images of resolution 3020×3020 at whose center FH center locates are imported into a CAD software, i.e., Solidworks 2015 (Dassault Systèmes, Vélizy-Villacoublay Cedex, France). With respect to the known diameter of FH, polyethylene wear was calculated as the change in the intercenter distance of the femoral head and the acetabular cup. And the lateral tilt of the acetabular cup was calculated as the angle between the horizontal line (i.e., medial-lateral line) and the line connecting the medial-most and lateral-most points (Fig. 7). The anteversion of AC calculated by the Lewinnek method¹¹. The true translation of FH was 6.67 mm, and the true lateral inclination and anteversion of AC were 36.6° and 9.0°, respectively.

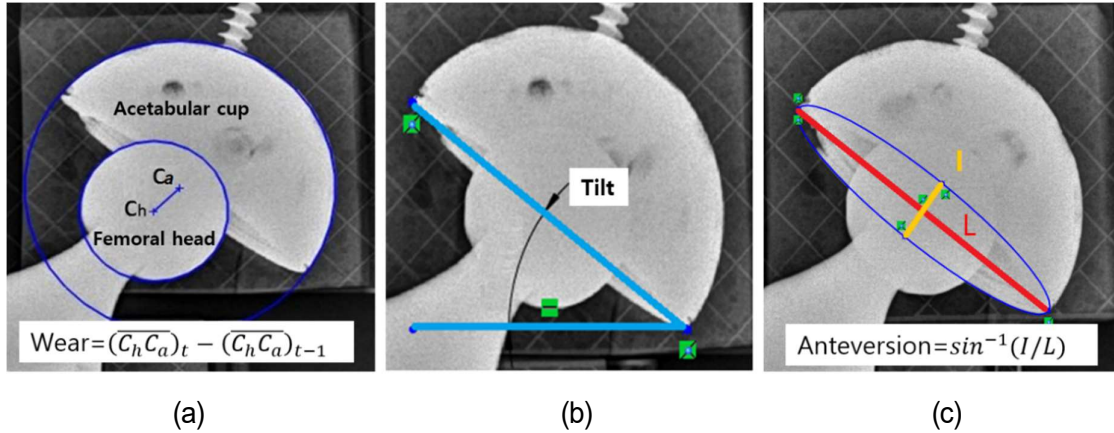


Fig 7. Measured values for Ployware evaluation. (a) Wear X-ray images of the initial (the left) and final (the right) positions, simulating the wear of the cup by a translation of the femoral stem of 6.67 mm normal to the equator plane of AC.

6.3. PW compatibility of X-ray image sizes

Image loading error

When loading the X-ray images into PW, all the X-ray images with a resolution of 3020×3020 or higher led to the generation of an error message. We term this error as the image loading error. The size of an image is determined by several parameters such as file format, the level of color/gray expression, and resolution. Because all the X-ray images in our study were TIFF format with a 256 grey level, the sole parameter that determined the image size was resolution. Various resolution images were tested to assess their compatibility to PW in the image loading step. The original X-ray image corresponded to a resolution of 3020×3020 and took FH located at the center of FH, and it was then downsized to various lower resolution images down to 1024×1024 (Table 2).

6.4 Effect of spatial eccentricity of the objects in original X-ray images

Test setups of the spatial eccentricity modes

As an object moves away from the center of the X-ray beam source on a vertical plane, the distance from the X-ray beam source to the object also increases, whereas the perspective viewing angle of the object

field decreases¹³. Thus, the silhouette shape of the object is projected differently on a detector plane, and PW measurement would return different measurement results. We defined the spatial eccentricity as the translational deviation of FH center from the center of the original X-ray image on the same plane normal to the vector passing the X-ray source and the detector centers.

Nine spatial eccentricity modes were set up via translating the THA prosthesis on the X-ray detector. With respect to the central location mode (O), other eight modes were specified via translating the prosthesis by 15 cm in left, right, superior, and/or inferior directions (Fig. 8). The central mode (O) represents that the center of a FH places at the center of an X-ray beam. The resolution of all the X-ray images used for the eccentricity tests was 1076×1076. At all the nine modes, the same wear of 6.67 mm was simulated without applying any rotation. Because the prosthesis was only translated without rotated at all the nine eccentricity modes, the angular alignments of AC and the wear of the acetabular liner should be measured into identical values, respectively.

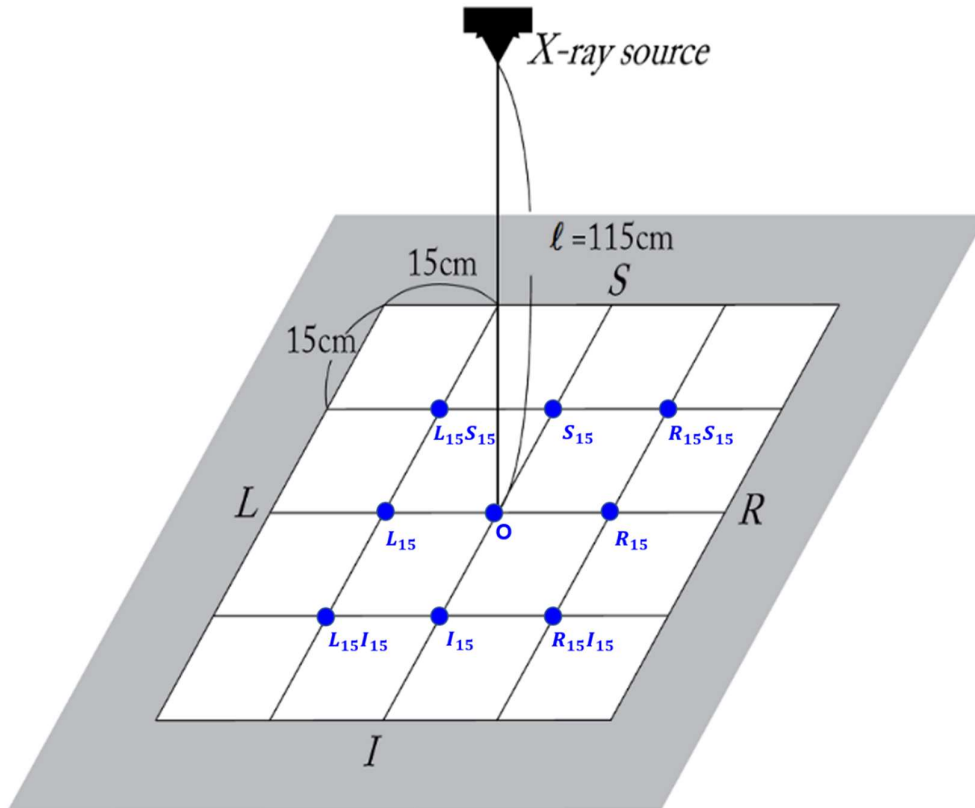


Fig 8. Eccentricity comparison test setup, i.e. nine spatial eccentricity modes. With respect to the center of the X-ray detector, nine spatial eccentricity locations of the THA prostheses were set up to figure out how the eccentricity of the component location affected PolyWare measurement results.

6.5. PW compatibility of geographical features of the user-specified edge detection area

In a set of PW analyses, the pre-process step termed as “a pre-process anteroposterior (AP) image” cuts out the unnecessary region from the initially loaded AP X-ray images for measurements. When a user assigns a rectangular area by dragging the mouse cursor from a point to its corresponding diagonal point, PW magnifies the inside of the rectangle into a full working window size. This step assigns only the necessary region for edge detection of FH and AC, for more precise and faster analysis. Then, PW executes edge detection for this rectangular area.

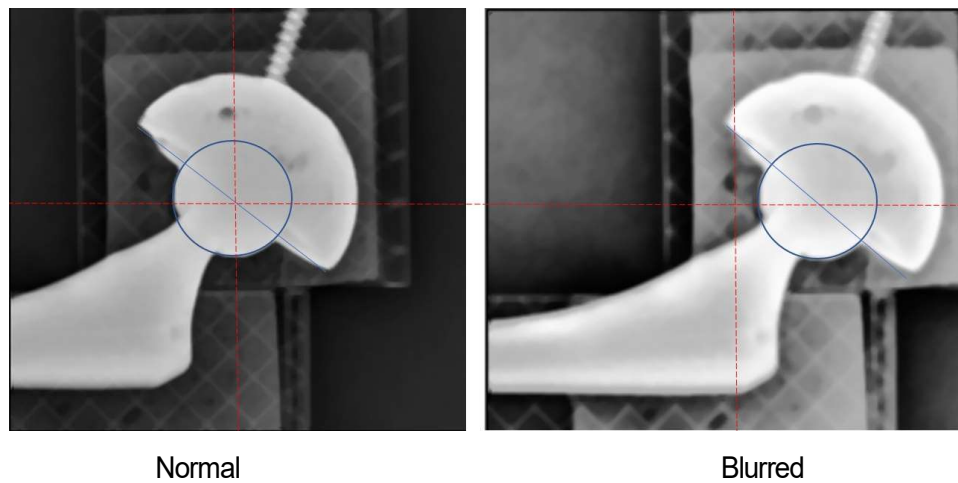


Fig 9. Blur of the edge detection area. For the same X-ray image, different specifications of rectangular edge detection areas result in different image sharpness. The left is shown normal, but the right is shown blurred. In the normal case, the rectangular edge detection area is specified such that its center positions at the very center of the femoral head. In the blurred case, in contrast, the rectangular edge detection area is specified such that its center positions considerably off the center of the femoral head, and the edge detection area becomes blurred.

Blur of the edge detection area

Even though images are loaded into PW without the image loading error, PW occasionally returns blur of the selected image region at the pre-process AP image step. The blur is intuitively recognized as in [Fig. 9](#). However, the condition in which the image blur occurs is unveiled. The normal imaging did not change its grey expression of the original X-ray image. In contrast, the blurred imaging changed the grey expression as

considerably whiter and blurry throughout the whole edge detection area.

To avoid the blur phenomenon, it was necessary to prevent the condition that brings about the blur. Numerous tests indicated that the location of the user-specified edge detection area sensitively affects the blur phenomenon. When the center of the detection area was specified more central to the FH center, the frequency of occurrence of the blur decreased. Hence, we hypothesized that the location of FH in edge detection area directly affects the image blur. Therefore, the following **three specifying configurations of the edge detection area** were compared (Fig. 10).

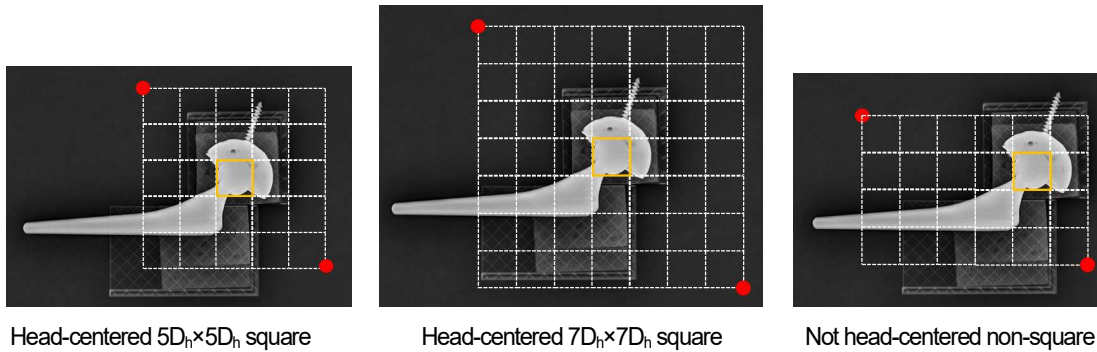


Fig 10. Three ways of specification of the edge detection area. Edge detection area assigned as a rectangle whose edge lengths were 5 times ($5D_h$) square, 7 times ($7D_h$) square of the diameter of the femoral head component (D_h), or non-square. The square areas specified were centered at the FH center, whereas non-square one off the FH center.

- **Head-centered $5D_h \times 5D_h$ square:** The first configuration is assigning the area as a square with edge lengths corresponding five times the diameter of FH (D_h) and centered at the center of FH component.
- **Head-centered $7D_h \times 7D_h$ square:** The second configuration is the same profile as that of the first method, although its edge lengths are seven times the diameter of the FH component (D_h).
- **Not head-centered non-square:** The last configuration is a random specification as neither square-shaped nor centered at FH center. The non-square specification indicates that the observer specifies the areas in non-squared rectangles and improvised sizes.

For this edge detection area specification test, X-ray images with a resolution of 1076×1076 were used. The image resolution of 1076×1076 was selected because it was found as the most compatible resolution to PW and is presented in the Results section.

Acknowledgement

This study is performed for solely research purpose and never supported by any commercial organizations or personals.

Authors' contributions

JM Lee performed experiments and data analysis, and SH Baek devised the motive of the study and participated in the manuscript writing. And YS Lee carried out experiments, the interpretation of results, and manuscript writing. All authors have read and approved the final submitted manuscript.

Funding

This study is supported by the research grant of National Research Foundation of Korea (2017R1A2B2005065). The grant has not taken any role besides financial support for the study.

Ethics approval and consent to participate

This manuscript has never been published before in any other form. And, this submission is carried out only to this journal, will never do to other journals during the review whole process. This study does not include any living subject's data.

Consent for publication

We read the copyright & publication policy of Nature Scientific Reports and agree on it.

Competing interests

The authors declare that they have no competing interests.

Availability of data and material

The raw image data and the experimental setup of this study are available from the corresponding author upon reasonable request.

References

1. Bozic, K. J. *et al.* The epidemiology of revision total hip arthroplasty in the United States. *JBJS* **91**, 128-133, doi:doi: 10.2106/JBJS.H.00155 (2009).
2. Shen, C. *et al.* Does cross-linked polyethylene decrease the revision rate of total hip arthroplasty compared with conventional polyethylene? A meta-analysis. *Orthopaedics & Traumatology: Surgery & Research* **100**, 745-750 (2014).
3. Biedermann, R. *et al.* Reducing the risk of dislocation after total hip arthroplasty: the effect of orientation of the acetabular component. *The Journal of bone and joint surgery. British volume* **87**, 762-769 (2005).
4. D'lima, D. D., Urquhart, A. G., Buehler, K. O., Walker, R. H. & Colwell Jr, C. W. The effect of the orientation of the acetabular and femoral components on the range of motion of the hip at different head-neck ratios. *JBJS* **82**, 315-321, doi:DOI: 10.2106/00004623-200003000-00003 (2000).
5. Dumbleton, J. H., Manley, M. T. & Edidin, A. A. A literature review of the association between wear rate and osteolysis in total hip arthroplasty. *The Journal of arthroplasty* **17**, 649-661 (2002).
6. Kennedy, J. *et al.* Effect of acetabular component orientation on recurrent dislocation, pelvic osteolysis, polyethylene wear, and component migration. *The Journal of arthroplasty* **13**, 530-534 (1998).
7. Kerrigan, C. S., McKenna, S. J., Ricketts, I. W. & Wigderowitz, C. Automated assessment of polyethylene wear in cemented acetabular components using anteroposterior radiographs of total hip replacements. *Computerized Medical Imaging and Graphics* **32**, 221-238 (2008).
8. Wan, Z., Boutary, M. & Dorr, L. D. The influence of acetabular component position on wear in total hip arthroplasty. *The Journal of arthroplasty* **23**, 51-56 (2008).
9. Shin, W. *et al.* The reliability and accuracy of measuring anteversion of the acetabular component on plain anteroposterior and lateral radiographs after total hip arthroplasty. *The bone & joint journal* **97**, 611-616 (2015).
10. Zheng, G. Effective incorporating spatial information in a mutual information based 3D-2D registration of a CT volume to X-ray images. *Computerized Medical Imaging and Graphics* **34**, 553-562, doi:<https://doi.org/10.1016/j.compmedimag.2010.03.004> (2010).
11. Lewinnek, G. E., Lewis, J., Tarr, R., Compere, C. & Zimmerman, J. Dislocations after total hip-replacement arthroplasties. *The Journal of bone and joint surgery. American volume* **60**, 217-220 (1978).
12. Park, Y. S. *et al.* The best method for evaluating anteversion of the acetabular component after total hip arthroplasty on plain radiographs. *Journal of orthopaedic surgery and Research* **13**, 66 (2018).
13. Kerr, D. A. The proper pivot point for panoramic photography. *The Pumpkin* **2**, 1-15 (2008).

Figures

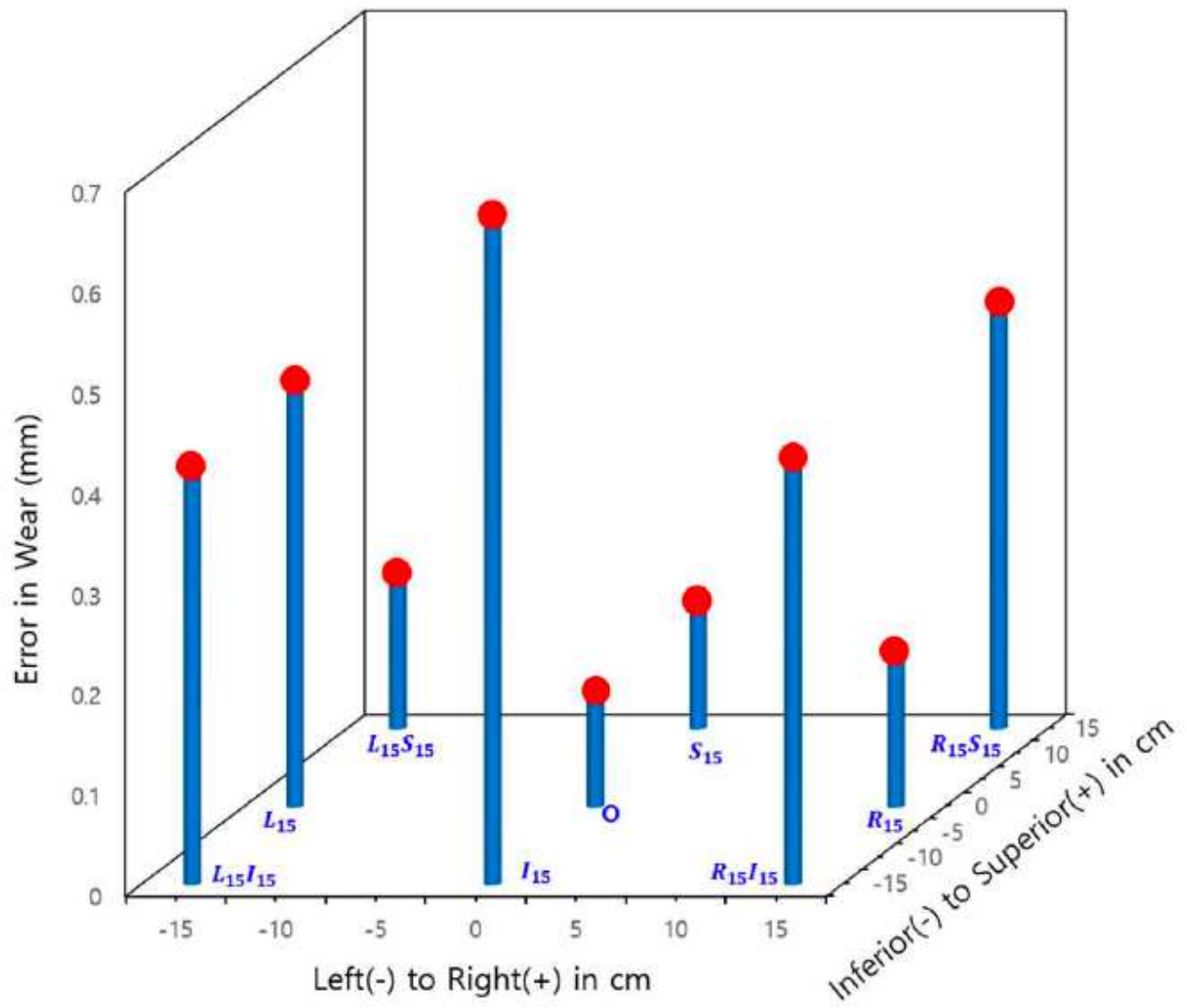


Figure 1

Error (in absolute value) in the wear for spatial eccentricity modes of the femoral head in the original X-ray images

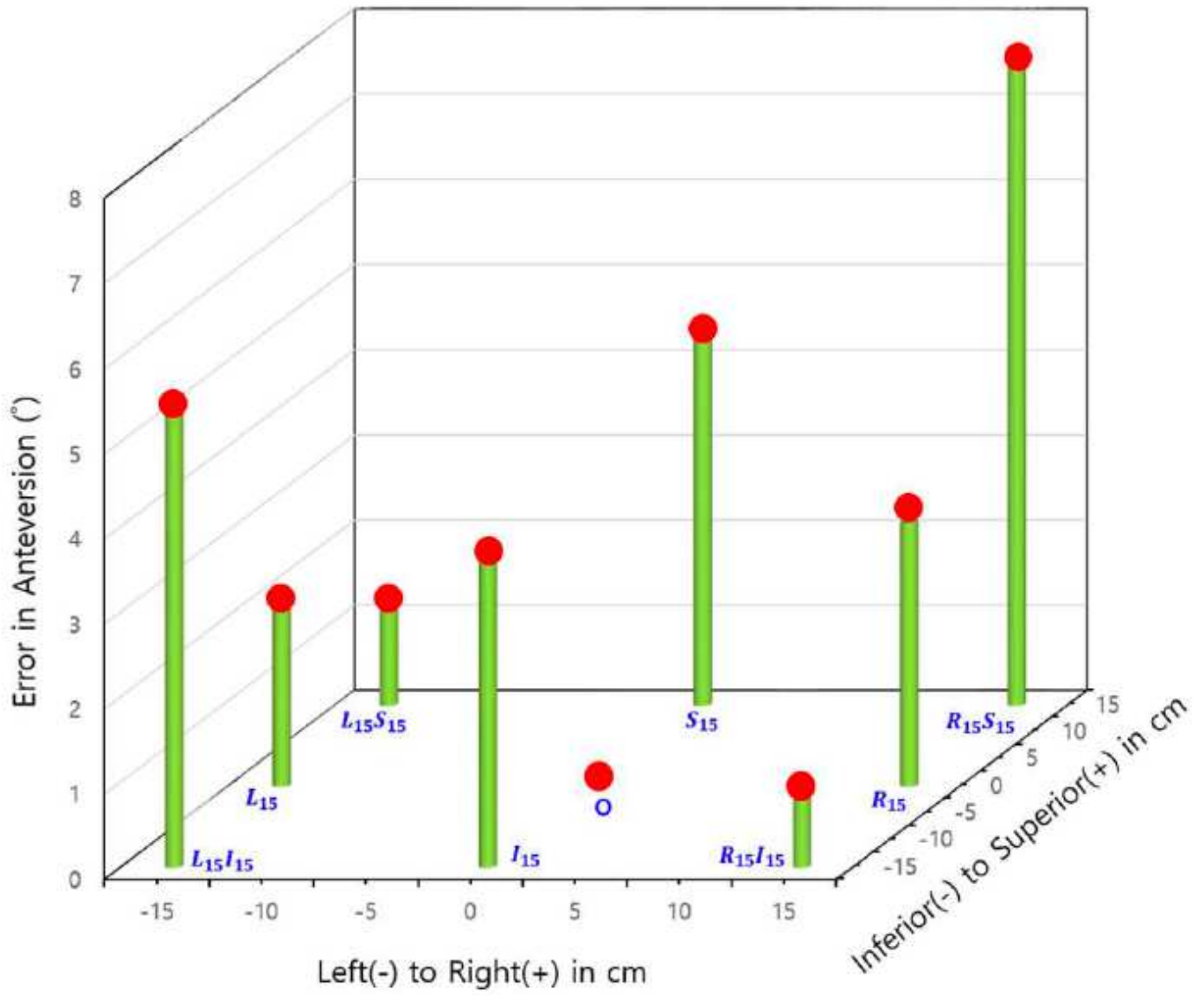
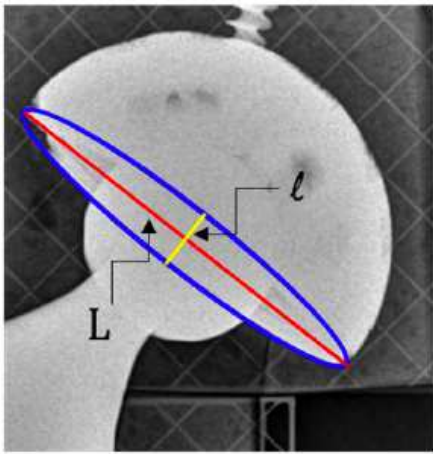
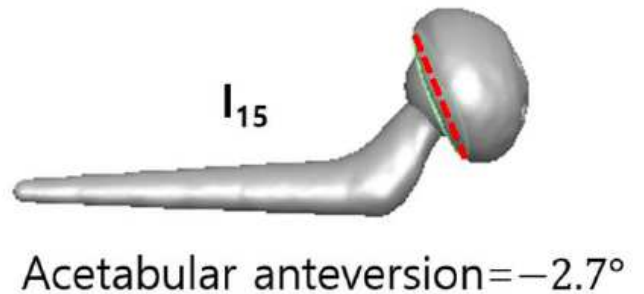
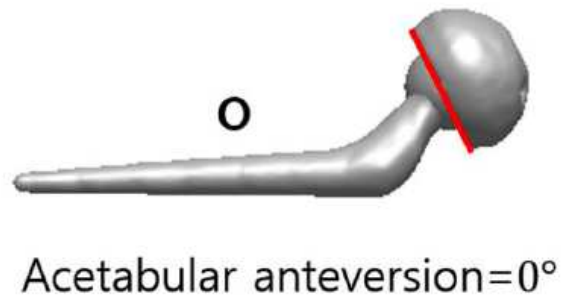
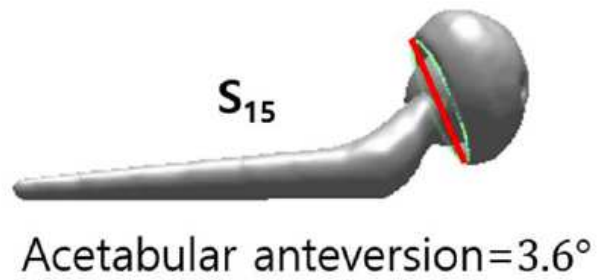
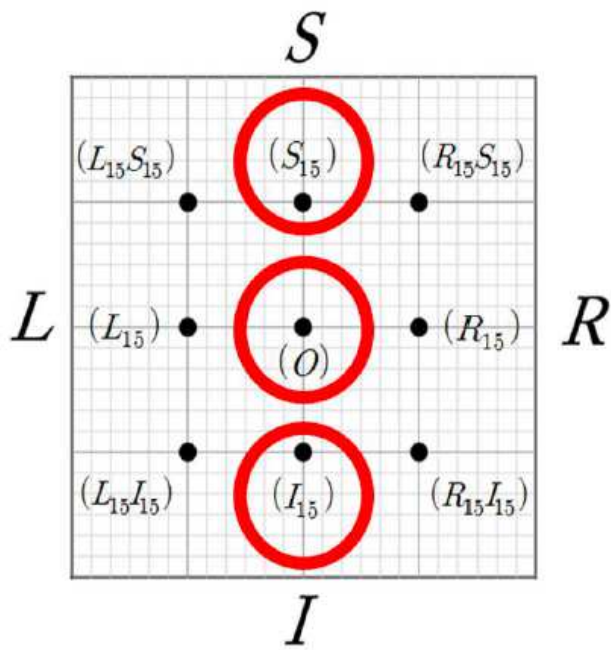


Figure 2

Errors (in absolute value) in the acetabular anteversion for spatial eccentricity modes of the femoral head in the original X-ray images



Acetabular anteversion = $\sin^{-1}\left(\frac{l}{L}\right)$
by Lewinnek[12]

Figure 3

Measurement of acetabular anteversion using a CAD to investigate the effect eccentricity of the prosthesis from the center of X-ray beam on the acetabular anteversion. The same X-ray images used for Polyethylene measurements were also used for the measurement using a CAD software, i.e. Rapidform 2006 ® (INUSTechnology, Seoul, Korea). The superior and inferior placements of the prosthesis bring about errors in acetabular anteversion, by the nature of perspective X-ray imaging.

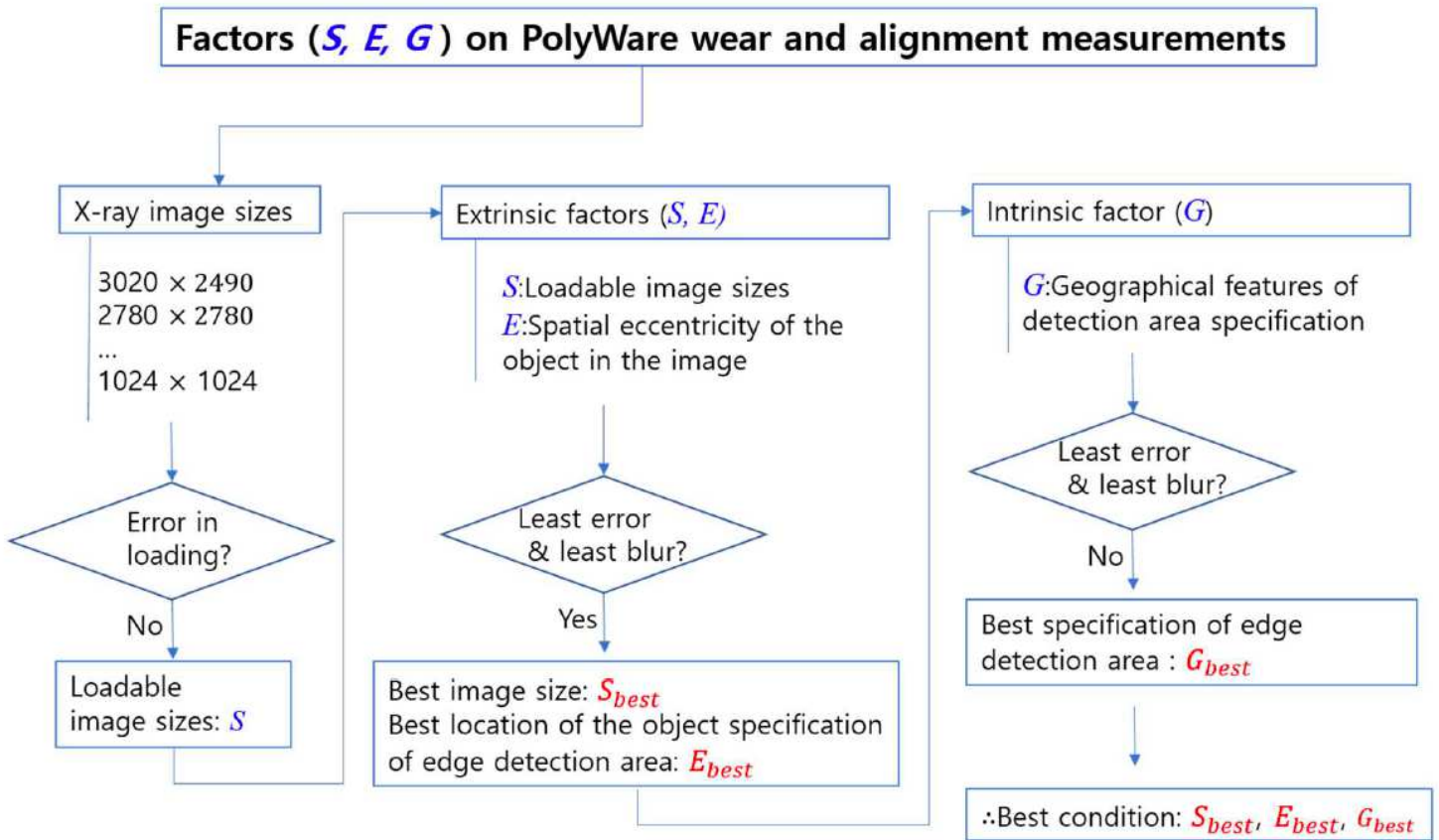


Figure 4

Overall process scheme of the current study

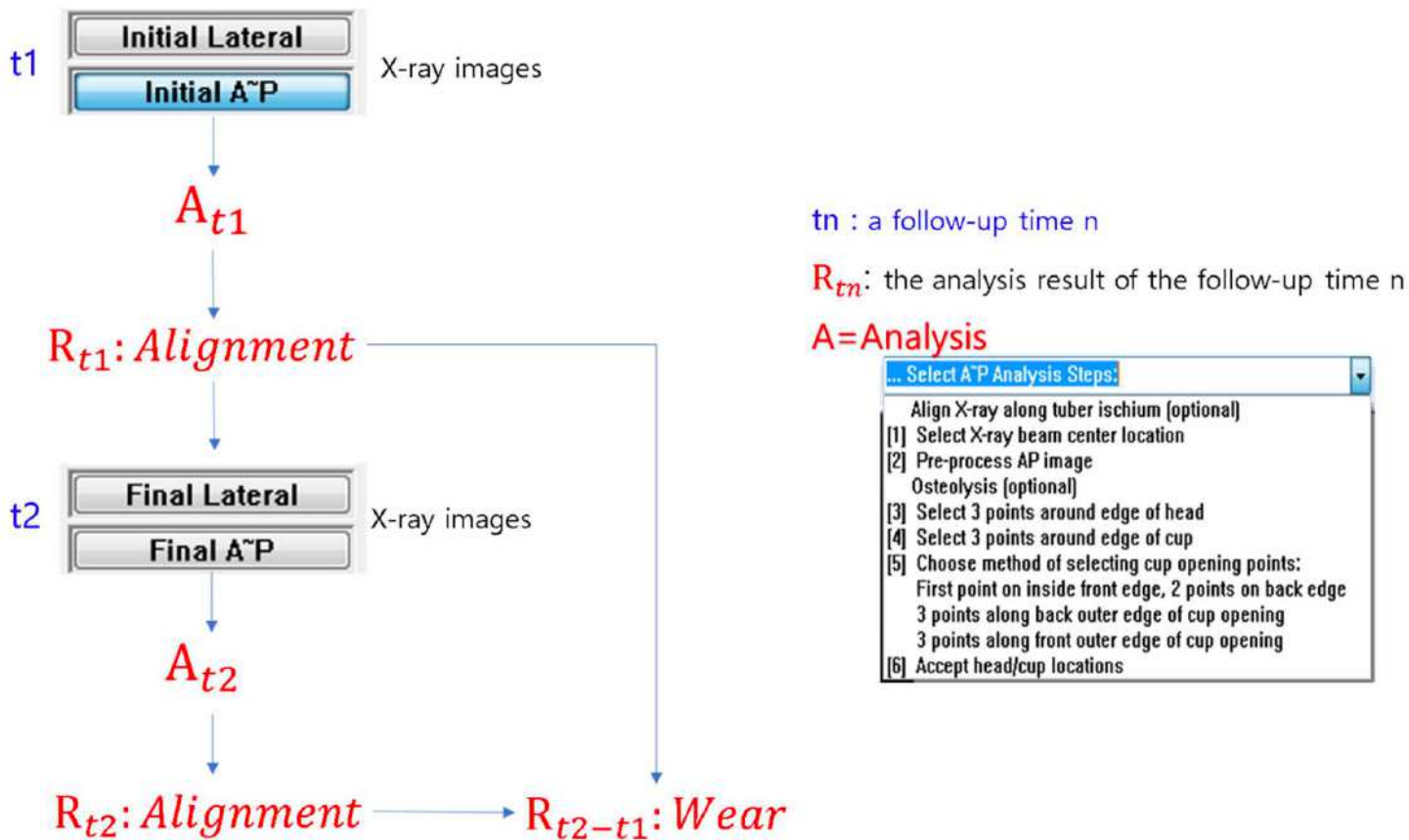


Figure 5

PolyWare work flow

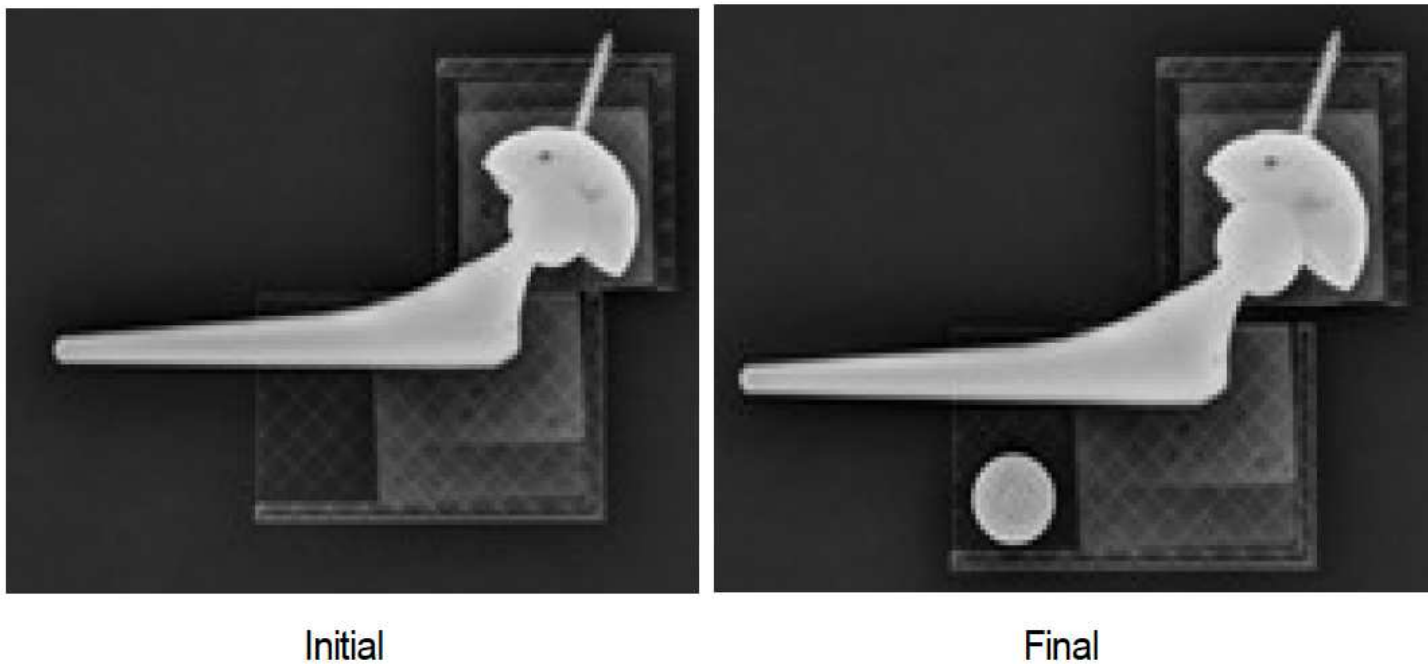


Figure 6

X-ray images of the initial (the left) and final (the right) positions, simulating the wear of the cup by a translation of the femoral stem of 6.67 mm normal to the equator plane of AC.

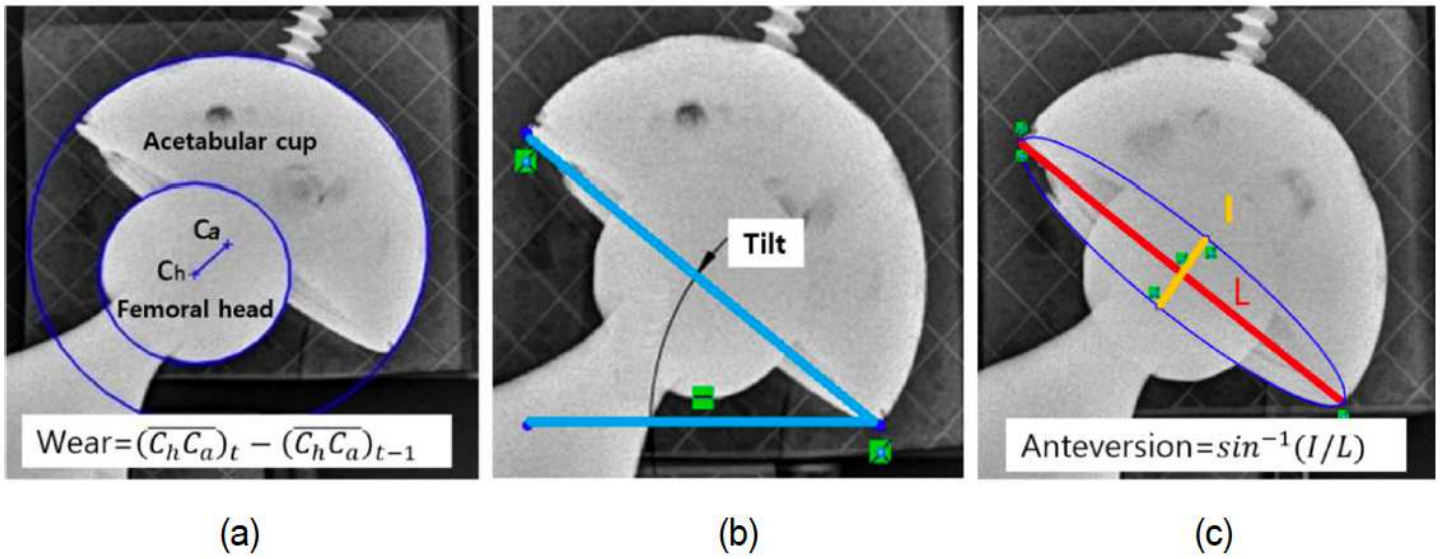


Figure 7

Measured values for Ployware evaluation. (a) Wear X-ray images of the initial (the left) and final (the right) positions, simulating the wear of the cup by a translation of the femoral stem of 6.67 mm normal to the equator plane of AC.

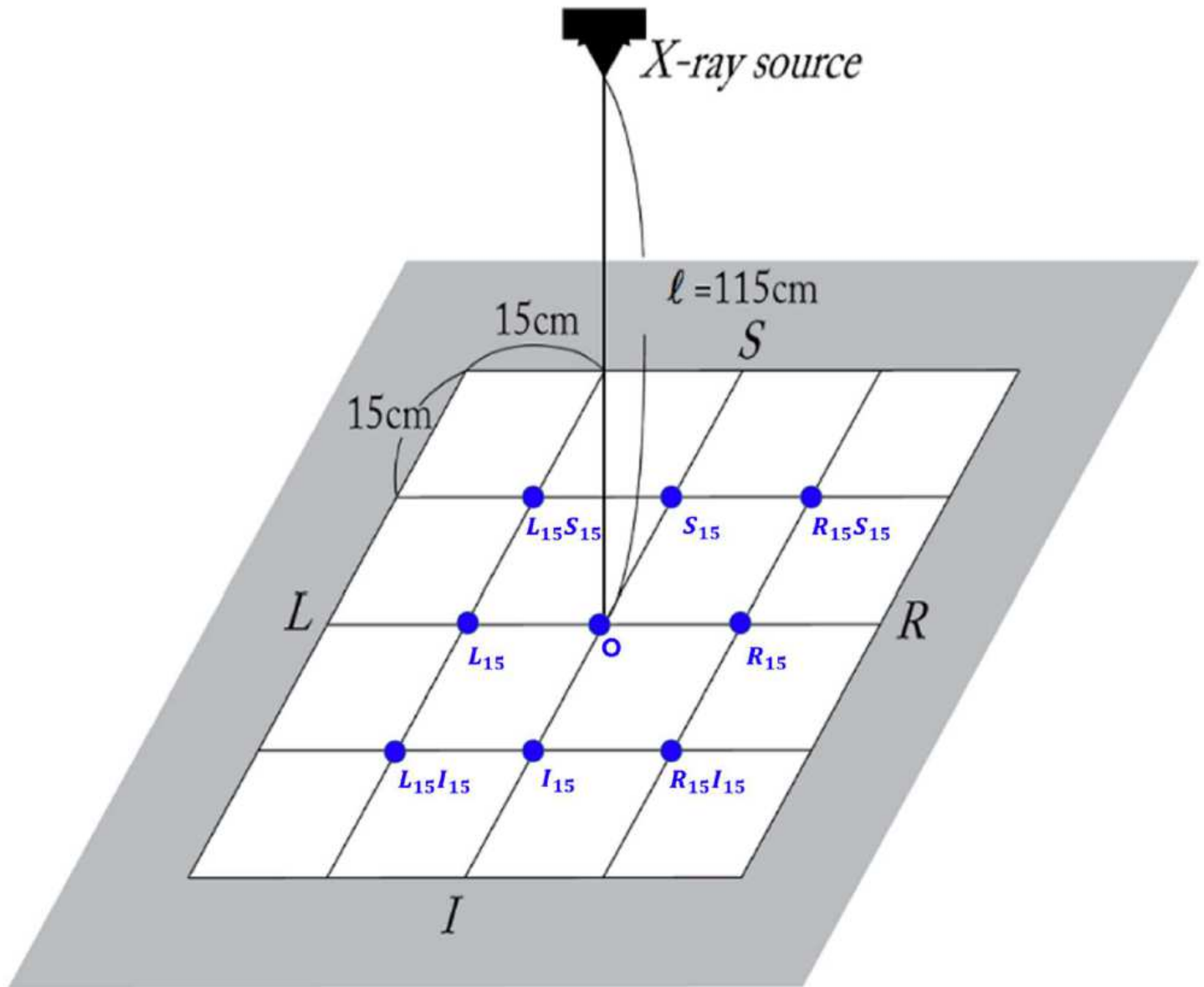
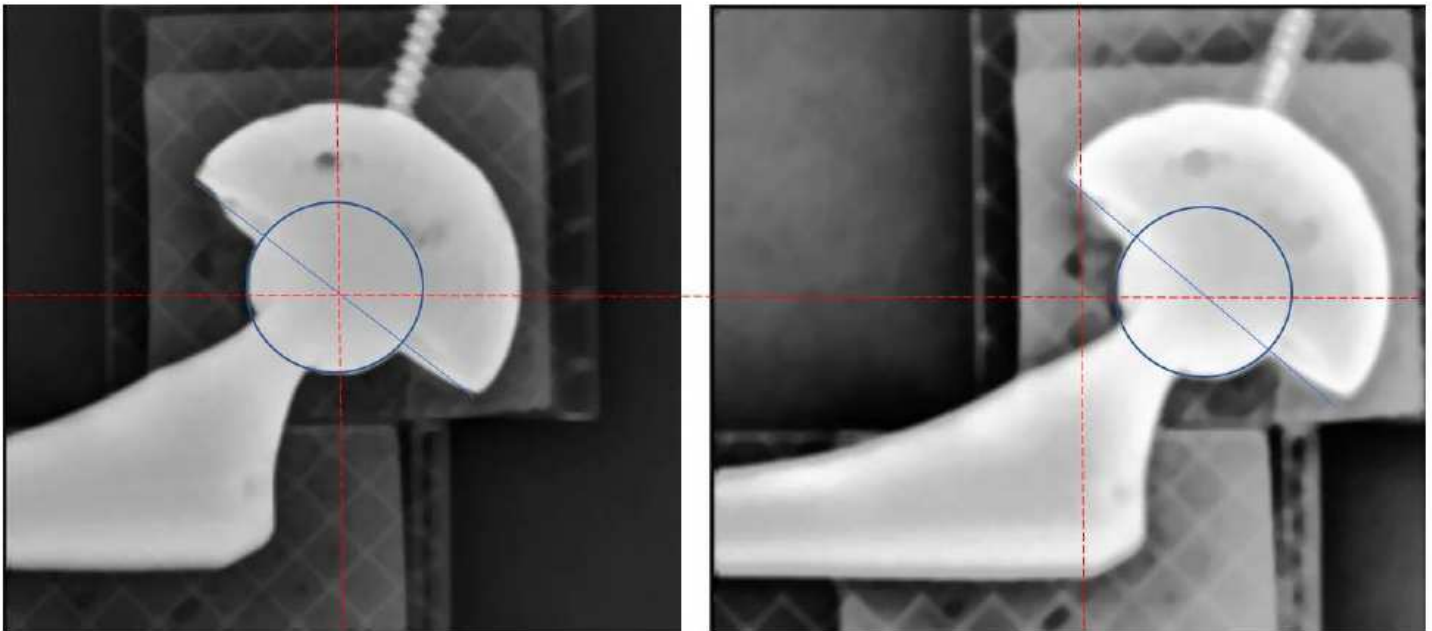


Figure 8

Eccentricity comparison test setup, i.e. nine spatial eccentricity modes. With respect to the center of the X-ray detector, nine spatial eccentricity locations of the THA prostheses were set up to figure out how the eccentricity of the component location affected PolyWare measurement results.

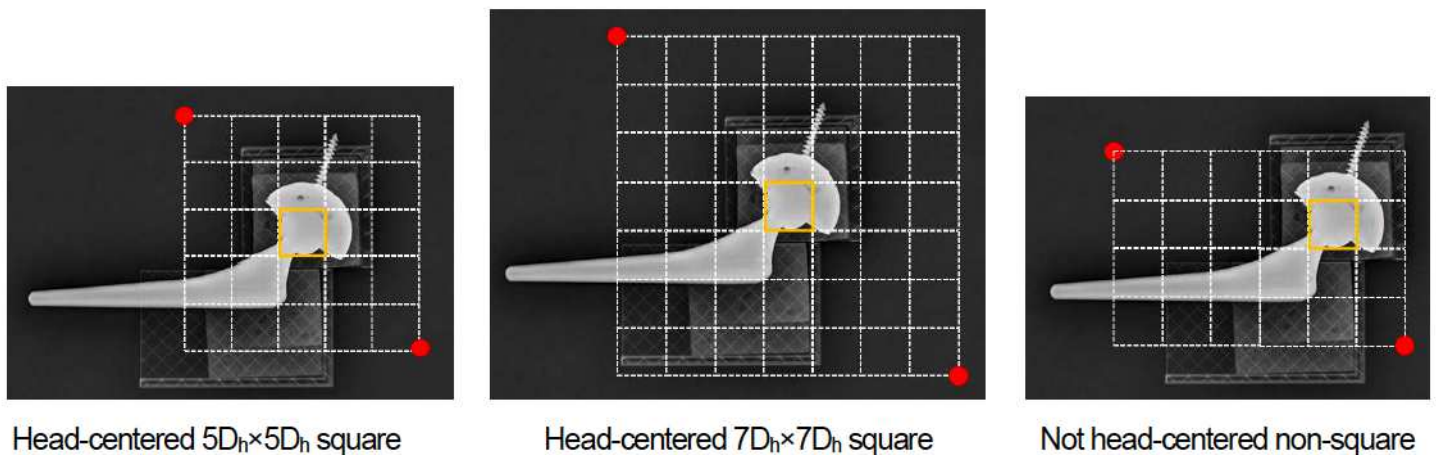


Normal

Blurred

Figure 9

Blur of the edge detection area. For the same X-ray image, different specifications of rectangular edge detection areas result in different image sharpness. The left is shown normal, but the right is shown blurred. In the normal case, the rectangular edge detection area is specified such that its center positions at the very center of the femoral head. In the blurred case, in contrast, the rectangular edge detection area is specified such that its center positions considerably off the center of the femoral head, and the edge detection area becomes blurred.



Head-centered $5D_h \times 5D_h$ square

Head-centered $7D_h \times 7D_h$ square

Not head-centered non-square

Figure 10

Three ways of specification of the edge detection area. Edge detection area assigned as a rectangle whose edge lengths were 5 times ($5D_h$) square, 7 times ($7D_h$) square of the diameter of the femoral head

component (Dh), or non-square. The square areas specified were centered at the FH center, whereas non-square one off the FH center.